Neurobiology of Disease

Peri-Infarct Depolarizations Reveal Penumbra-Like Conditions in Striatum

Masao Umegaki,[1,2]* Yasuhiro Sanada,[1,2]* Yannic Waerzeggers,[1] Gerhard Rosner,[1] Toshiki Yoshimine,[2] Wolf-Dieter Heiss,[1] and Rudolf Graf[1]

[1]Max-Planck Institute for Neurological Research, D-50931 Köln, Germany, and [2]Department of Neurosurgery, Osaka University Graduate School of Medicine, Osaka 565-0871, Japan

Spreading depression-like peri-infarct depolarizations not only characterize but also worsen penumbra conditions in cortical border zones of experimental focal ischemia. We intended to investigate the relevance of ischemic depolarization in subcortical regions of ischemic territories.

Calomel electrodes measured DC potentials simultaneously in the lateral and medial portions of the caudate nucleus (CN) of 11 anesthetized cats after permanent occlusion of the middle cerebral artery. Additionally, platinum electrodes measured cerebral blood flow (CBF) in the CN, and laser Doppler probes CBF in the cortex.

Depolarizations (negative DC shifts >10 mV) were obtained in 10 of 11 cats. Further differentiation revealed that short-lasting spreading depression-like depolarizations (SDs; 5 of 10 cats: 5.24 ± 1.22 min total duration; 23.3 ± 4.2 mV amplitude) were predominantly found in medial and longer depolarizations (LDs; 4 of 10 cats: 64.7 ± 47.5 min; 25.0 ± 11.3 mV) in the lateral CN. Terminal depolarizations (TDs; 6 of 10 cats; without repolarization) occurred immediately after occlusion or at later stages, being then accompanied by elevations of intracranial pressure presumably inducing secondary CBF reduction. CBF tended to be lower in regions with TDs (33.3 ± 29.9% of control) and LDs (37.3 ± 22.8%) than in regions with SDs (51.5 ± 48.0%).

We conclude that in focal ischemia, transient peri-infarct depolarizations emerge not only in cortical but also in striatal gray matter, thereby demonstrating the existence of subcortical zones of ischemic penumbra. The generation of these ischemic depolarizations is a multifocal process possibly linked to brain swelling and intracranial pressure rise in the later course of focal ischemia, and therefore a relevant correlate of progressively worsening conditions.

Key words: **peri-infarct depolarization; spreading depression; focal ischemia; intracranial pressure; striatum; cat**

Introduction

Approximately 60 years ago, the Brazilian physiologist Leão (1944) described cortical spreading depression (CSD) as a transient, wave-like reduction of electroencephalographic activity that goes along with a negative deflection of the cortical DC potential and marked alterations in extracellular and intracellular ion concentrations. It may be triggered by a variety of external stimuli such as high extracellular K^+ or glutamate and moves slowly across the cerebral cortex (for review, see Marshall, 1959; Bureš et al., 1974; Somjen, 2001).

In the last decade, the phenomenon has attracted renewed attention because it has become clear from experimental work that intrinsic pathophysiological conditions such as brain trauma (Nilsson et al., 1993) or focal ischemia (Strong et al., 1983; Nedergaard and Astrup, 1986; Nedergaard and Hansen, 1993) generate recurrent waves of CSD. Furthermore, a recent electrophysiological study on trauma patients has provided evidence for a role of CSD in the pathophysiology of border zones of injured tissue in humans (Strong et al., 2002). Likewise, a functional magnetic resonance imaging (MRI) study on migraine patients has presented data suggesting that CSD generates the migraine aura in human visual cortex (Hadjikhani et al., 2001).

Most probably, CSD contributes to progressive deterioration in peri-infarct zones of ischemic foci, being then called peri-infarct depolarizations (Mies et al., 1993; Back et al., 1994; Hossmann, 1996; Saito et al., 1997; Strong et al., 2000; Ohta et al., 2001). Differences between CSD and peri-infarct depolarization concern particularly compensatory hyperemia, which is typical for CSD in healthy tissue but is reduced or missing during peri-infarct depolarization (Back et al., 1994). Each recurrent wave of depolarization may thereby result in stepwise, progressive ATP depletion and functional as well as structural deterioration (Busch et al., 1996; Röther et al., 1996; Ohta et al., 2001; Higuchi et al., 2002). Terminal depolarization (TD) and destruction of penumbral tissue may mark an end point of this process (Hossmann, 1996).

Because focal ischemia is not restricted to cortical regions, we

Received Oct. 8, 2004; revised Dec. 21, 2004; accepted Dec. 21, 2004.

This work was supported by a grant from the Bundesministerium für Bildung und Forschung (Kompetenznetz Schlaganfall) to R.G. and W.-D.H. We thank Doris Lattacz, Andreas Beyrau, and Bernd Radermacher for valuable technical assistance.

*M.U. and Y.S. contributed equally to this work.

Correspondence should be addressed to Dr. Rudolf Graf, Max-Planck-Institut für neurologische Forschung, Gleueler Strasse 50, D-50931 Köln, Germany. E-mail: rudolf.graf@pet.mpin-koeln.mpg.de.

DOI:10.1523/JNEUROSCI.4182-04.2005

 0270-6474/05/251387-08$15.00/0

intended to find out whether in the process of progressive infarction, peri-infarct depolarization occurs in other brain regions as well. In our previous studies in a model of middle cerebral artery occlusion (MCAO) in cats, we have shown stepwise, progressive cortical deterioration with recurrent depolarizations (Ohta et al., 2001). We now succeeded in the same model to detect peri-infarct depolarizations in the caudate nucleus. Here, we show recordings and characterize profiles of various types of ischemic depolarization in the striatum, compare its appearance with that in the cortex, and discuss its significance for the pathological process and the existence of an ischemic penumbra in the striatum.

Materials and Methods

Eleven adult cats of both sexes weighing 2.8–5.1 kg were used. The study was approved by the local Animal Care Committee and Regierungspräsident of Köln and is in compliance with the German Laws for Animal Protection. General anesthesia was initialized with ketamine hydrochloride (25 mg/kg, i.m.). The left femoral vein and artery were cannulated to administer drugs and to measure mean arterial blood pressure (MABP) and arterial blood gases, and the animals were tracheotomized and immobilized with pancuronium bromide (0.2 mg/kg, i.v.). Artificial ventilation was started, and anesthesia was changed to halothane (0.6–1.2%) in a 70% nitrous oxide/30% oxygen gas mixture. Ringer's solution containing gallamine triethiodide (5 mg/kg/h) was infused intravenously (3 ml/h) for immobilization throughout the experiment. Artificial ventilation was controlled, keeping arterial and expiratory gases within normal physiological ranges. Deep body temperature was maintained at 37°C using a heating blanket feedback controlled by a rectal temperature probe.

The left MCA was exposed transorbitally. A device for remote occlusion (Graf et al., 1986; Ohta et al., 1997) was implanted at the proximal portion of the MCA between the left optic nerve and the MCA bifurcation. The device was completely fixed with gelfoam and rapid-drying glue. Finally, the orbit was sealed with dental cement to avoid CSF leakage and to make again the intracranial space a closed system.

We used microelectrodes [glass capillary micropipettes filled with 10% NaCl solution (tip diameter, 2–4 μm), in which a miniature calomel electrode had been inserted to avoid polarization] (Shibata et al., 1977) for DC and EEG recordings. We attached platinum microelectrodes (etched platinum iridium wires 250 μm in diameter; glass insulated up to 1 mm of the tip) to the micropipettes at 1–2 mm distance for measurement of regional cerebral blood flow (CBF) using hydrogen clearance. Pairs consisting of the two types of electrodes were mounted in a self-made micromanipulator that allowed independent movement of single pairs of electrodes. EEG and DC potentials were recorded using differential amplifiers with appropriate filtering (EEG: high-pass, 0.5 Hz; low-pass, 50 Hz; DC potential: low-pass cutoff at 0.1 Hz). A calomel electrode inserted under the skin in the nasal region served as an indifferent reference. For hydrogen clearance, monopolar recordings were performed using a separate set of amplifiers.

To approach the caudate nucleus, a 6-mm-diameter burr hole was drilled in the left skull at stereotaxic coordinates 17 mm anterior/4 mm lateral (Reinoso-Suarez, 1961). After careful dura incision, two sets of the described electrode pairs were inserted in the same coronal plane, one into a medial portion (17 mm anterior/2 mm lateral; 12–14 mm deep from brain surface) and the other into a lateral portion (17 mm anterior/6 mm lateral; 11–12 mm deep) of the left caudate nucleus (Fig. 1). The tip-to-tip distance of the electrode pairs was ~4 mm. Thereafter, a smaller burr hole was drilled in the skull above the left ectosylvian gyrus, and a laser Doppler flow (LDF) probe (tip diameter, 0.8 mm; Moor Instruments) was placed on the dura using a micromanipulator to measure the effect of MCAO. Additionally, a small burr hole was drilled in the skull above the right marginal gyrus, and after careful dura incision, a strain-gauge MicroSensor probe for measurement of intracranial pressure (ICP; Codman/Johnson & Johnson Professional, Randolph, MA), and a thermocouple for measurement of regional brain temperature were placed on the cortical surface. After positioning all the devices, the burr holes were completely sealed with gelfoam and dental cement to prevent CSF leakage. After preparation of the animals, a bolus of α-chloralose (60 mg/kg, i.v.) was administered, halothane was switched off, and artificial ventilation was kept at 70% nitrous oxide/30% oxygen. To keep α-chloralose anesthesia throughout the experiment, continuous α-chloralose infusion (5 mg/kg/h) was started ~3 h after the initial bolus had been injected. Experimental protocols were not started before at least 2 h after the initial α-chloralose injection had passed.

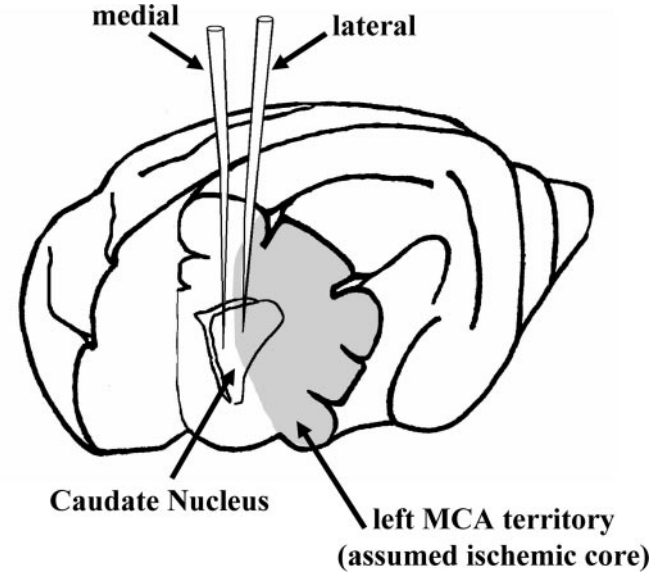

Figure 1. Schematic representation of recording sites in relation to the caudate nucleus and MCA territory. According to a stereotaxic atlas (Reinoso-Suarez, 1961), two miniature calomel electrodes (tip diameter, 2–4 μm) were vertically inserted into the left caudate nucleus in the same coronal plane at a distance of ~4 mm. We assumed that the lateral electrode was positioned more in the core and the medial electrode more in the rim of the ischemic focus. Adjacent to calomel electrodes, platinum electrodes measured CBF using hydrogen clearance.

Table 1. Physiological variables

	MABP (mmHg)	PaO_2 (mmHg)	$PaCO_2$ (mmHg)	pH
Before MCAO	161.6 ± 19.8	138.1 ± 21.7	33.5 ± 7.3	7.362 ± 0.039
Approximately 1 h after MCAO	159.0 ± 13.1	136.3 ± 33.8	36.3 ± 7.1	7.324 ± 0.050
Approximately 12 h after MCAO	142.7 ± 12.1	128.0 ± 32.3	37.6 ± 7.3	7.317 ± 0.077

Values are mean ± SD. Differences between different time points were not significant (repeated-measures ANOVA).

The experimental protocol was started with control measurements. All parameters besides hydrogen clearance (EEG, DC potential, CBF measured with LDF, ICP, ABP, and brain temperature) were recorded continuously. Regional CBF was measured before MCAO, immediately after MCAO, and several times in the course of the experiment until 12 h after MCAO. The experiments were continued for 12 more hours, so that a total experimental protocol of >24 h was followed. Experiments were terminated by intravenous injection of KCl. Data were recorded and analyzed using a personal computer-based data acquisition system (DASYLab; DASYTEC) and a statistics software (Statistica; StatSoft). Statistical evaluation was performed as indicated in the text.

Results

Physiological variables

The experimental protocol including the occlusion of the MCA did not significantly alter physiological variables such as blood gases and MABP (Table 1).

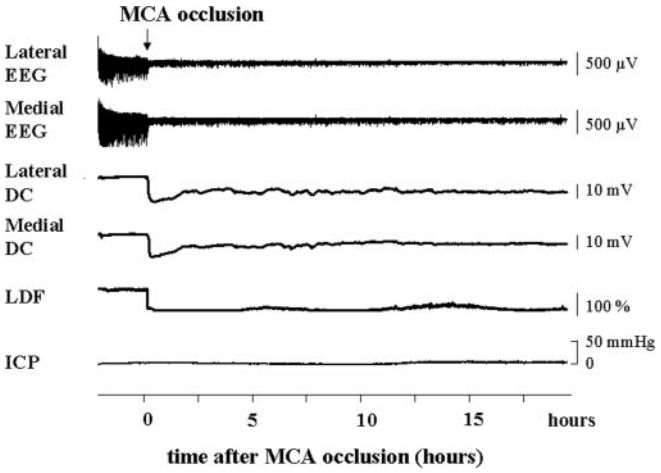

Figure 2. Simultaneous original recordings of ICP, DC potential, EEG in the lateral and medial caudate nucleus, and LDF in the cortex before and after permanent MCAO. Note the abrupt reduction of LDF in the cortex and immediate persistent depolarization at both recording sites in the caudate nucleus. ICP did not rise in this particular experiment.

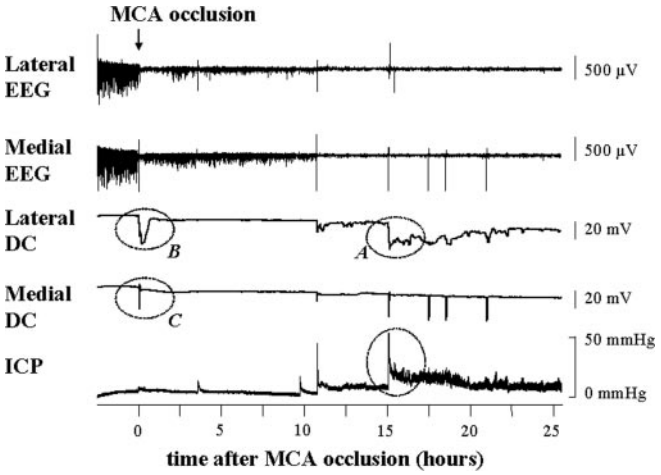

Figure 3. Simultaneous original recordings of ICP, DC potential, and EEG in the lateral and medial caudate nucleus before and after permanent MCAO. LDF in the cortex was not shown in this particular experiment because of technical problems with recording. Note the different types of depolarization at the circled segments A (TD), B (LD), and C (SD). Magnified cutouts of these segments are shown in Figure 4. In the lateral caudate nucleus, depolarization at A does not recover over several hours and is therefore defined as TD. The latter may be initiated by the stepwise increase of ICP at the same time point. In the medial caudate nucleus, repetitive waves of SD appear in the later course of the experiment exactly after TD in the lateral part.

Cortical blood flow

Effective MCAO was confirmed in all cats with cortical LDF measurements in a typical core region of the focal ischemia model in cats, the left ectosylvian gyrus (see examples in Figs. 2 and 6). The average CBF reduction in the ectosylvian gyrus immediately after MCAO amounted to 11.4 ± 8.54% of control (range, 2.9–33.3%). After this rather dramatic drop of CBF, we regularly observed in this region partial spontaneous reperfusion probably resulting from the opening of collateral channels (see in particular the example in Fig. 6).

Incidence and characterization of striatal depolarizations

DC recordings in the caudate nucleus uncovered persistent as well as transient types of depolarization after MCAO, examples of which are given in recordings in Figures 2–4.

Terminal depolarization

The first type of depolarization, referred to as TD, was persistent in nature and resembled anoxic depolarization. TD appeared, in some instances, immediately after MCAO, in one animal simultaneously at both recording sites in the striatum (see examples of lateral and medial EEG and DC recordings in the lateral and medial caudate nucleus in Fig. 2), documenting for a given region gross reduction of spontaneous electroencephalographic activity and presumably immediate severe disturbance of ion homeostasis caused by critical reduction of CBF. A sharp negative shift of −10 mV or more typically characterized the depolarization phase of TD. Thereafter, depolarization slowed down but continued to decrease for several minutes until it reached a minimum of approximately −20 mV. In the following period, the DC potential typically increased to some extent, often over hours. As a main characteristic, the negative shift of the DC potential in TD lasted >180 min, and it never reached the pre-depolarization baseline again. In other instances (A in Fig. 3), TD appeared later in the course of ischemia. Sometimes it fluctuated during this phase, as shown in the example. The concomitant appearance of the DC shift with a steep increase in ICP (A in Fig. 3) indicates that ICP elevations may be involved in the induction of such delayed TDs. An enlarged view of the recording (Fig. 4*A*) underscores that the now visible biphasic pattern of ICP elevation has a biphasic, shoulder-like correlate in the negative DC shift. In fact, a preceding smaller deflection of the DC potential (Fig. 3, lateral DC) seemed to be also caused by a concomitant smaller ICP rise documenting the close relationship between harmful development of elevated ICP and secondary induction of depolarizations.

Long depolarization

Another type of depolarization referred to as long depolarization (LD), was transient in nature but prolonged (B in Fig. 3; enlarged image in Fig. 4*B*). The first portion of the negative DC shift was relatively slow, followed by a steep drop. After the steep decline, we regularly observed an intermediate small increase in potential resulting in a shoulder-like appearance, followed by an additional slow decline to the minimum value. In LD, minimal values reached after several minutes were also in the range of −20 mV, and subsequent repolarization was slow. LD appeared both at the onset and in the later course of ischemia. In the given example (Fig. 4*B*), the minimum was reached after >15 min, and its whole duration was in the range of 40 min.

Spreading depression

A second, often recurrent type of transient depolarization, referred to as spreading depression (SD), resembled the phenomenon described first by Leão (1944). SD was much faster, with a total duration of typically <5 min (as an example, see C in Fig. 3; Fig. 4*C*). A very brief slow decrease at the beginning followed by a steep decline characterized the negative shift of approximately −20 mV of this type. Interestingly, the steep portion of the decline was comparable in shape with those observed in LD and TD (Fig. 4). Repolarization was typically slower than depolarization but fast compared with repolarization in LDs and passed into hyperpolarization before returning to pre-depolarization baseline levels. SDs are most probably propagated waves of depolarization. In the example shown in Figure 4 (bottom two panels), we compared the starting points S and also the steep portions of the decline of the LD and SD waves. If we assume that the SD is a propagated wave originating from the LD wave, which is presumably generated in the ischemic core, we can deduce from the distance of 4 mm between the two electrodes a propagation ve-

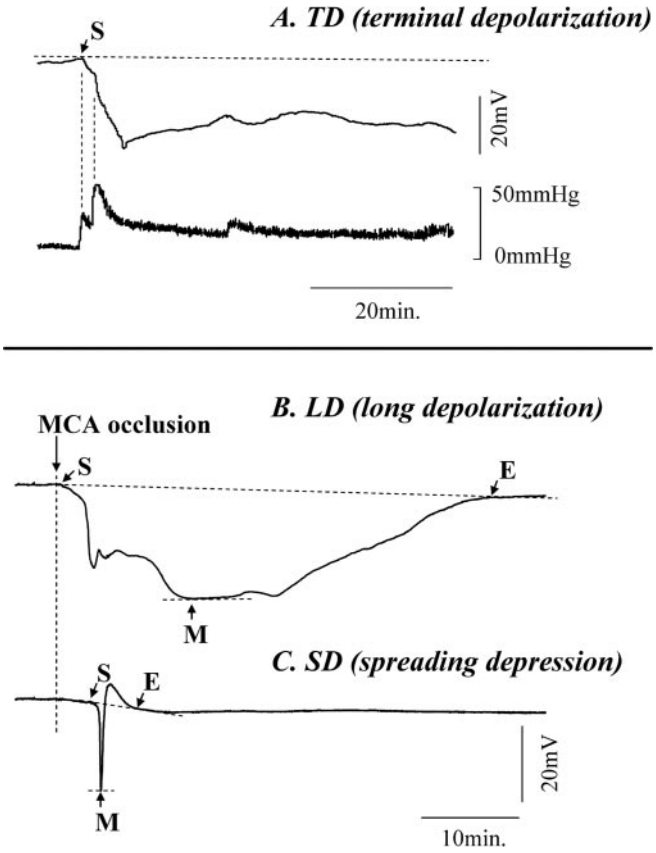

Figure 4. Magnified cutouts of DC recordings at segments A (with concomitant recording of ICP), B, and C from Figure 2 showing different types of depolarization in the caudate nucleus and the relationship of TD to increase of ICP after MCAO. Top, TD appearing in the later course of the experiment in the lateral caudate nucleus. Note the biphasic increase of ICP and the almost simultaneous biphasic, shoulder-like decrease of the DC potential. Bottom, Temporal relationship between LDs initiated by MCAO in the lateral caudate nucleus and a wave of SDs in the medial caudate nucleus. Note in the bottom panel the time lag between waves of LD and SD. SD has presumably propagated from the ischemic core in the lateral caudate nucleus to the ischemic rim in the medial caudate nucleus. Calculation of the latency between the steep declines of the DC potential in B and C revealed a propagation velocity of ~3 mm/min. Waves of depolarization have been analyzed using starting point S, end point E, and minimal value M.

locity of ~3 mm/min. This is well in the range of what has been described for SD propagation. No SDs were observed on the medial channel in the absence of depolarization first occurring on the lateral channel. In the few cases of SDs recorded on the lateral channel (2 of 19), we were not able to demonstrate preceding LD or TD in the medial portion of the caudate nucleus.

Temporal manifestation of striatal depolarizations

A total of 40 depolarizations were depicted in the 11 experiments, including 12 TDs, 9 LDs, and 19 SDs. Most of SDs (17 of 19) appeared on the medial electrode, whereas LDs (6 of 9) and TDs (8 of 12) appeared more often on the lateral electrode. Interestingly, the temporal appearance of depolarizations showed a biphasic pattern (Fig. 5). The first phase, with the exception of one SD, started within 10 min after MCAO, and the second phase followed ~10 h later.

Duration and amplitude of striatal depolarizations

The duration of SDs and LDs was assessed by measuring the time to maximal depolarization (Fig. 4, S–M) and the repolarization (Fig. 4, M–E) time. Based on combined depolarization and repolarization phases, the mean duration of SDs (5.2 ± 1.2 min) was

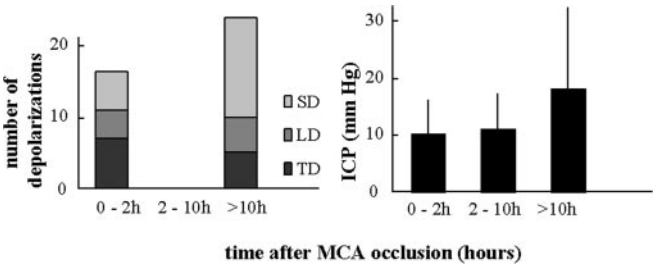

Figure 5. Temporal distribution of different types of depolarization (SD, LD, and TD; see Fig. 4) after MCAO and of according mean values (±SD) of ICP. Note that almost all depolarizations appeared either within the first 10 min or later than 10 h after MCAO. LDs as well as TDs in the later stage of experiments were always associated with increases of ICP, presumably resulting in secondary severe CBF reduction.

significantly shorter than that of LDs (64.8 ± 47.5 min; $p < 0.05$; *t* test). The amplitudes of the three types of depolarization were all in the same range of 10–30 mV, which is in accordance with reported values (for review, see Somjen, 2001; Gorji, 2001). In Table 2, the mean duration and amplitude of the various types of depolarization are listed for early and late phases. These values show that LDs in the late phase (later than 10 h after MCAO) are more variable than depolarizations at other time points.

Striatal electroencephalographic activity

The EEG amplitude in striatum decreased in all cats after MCAO. Original recordings obtained with the same electrodes that were used for DC recordings are given in Figures 2 and 3 for both the lateral and medial portion of the caudate nucleus. In the first example (Fig. 2), the EEG decreased substantially immediately after occlusion, and deterioration proceeded throughout the observation period, paralleling the consistent negative shift of the DC potential. In the second example (Fig. 3), the EEG was also suppressed almost immediately after occlusion but recovered thereafter to some extent, the recovery being faster and more pronounced in the medial recording site. This development corresponded to DC potential recordings in that the lateral site showed the more severe and longer-lasting LD compared with the short SD in the medial site. Mean EEG amplitude reductions in the caudate nucleus immediately after MCAO amounted to 24 ± 8, 26 ± 5, and 35 ± 7% of control on electrodes displaying TDs, LDs, and SDs, respectively. Differences between medial and lateral regions were not significant. Further EEG suppression with single SD waves was hardly to be observed in striatal recordings. We were also not able to detect in the striatum progressive, stepwise deterioration observed as a stepwise loss of the ability for restoration of EEG activity associated with recurrent waves of SD. Such observation was typical for cortical recordings obtained in the same model and provided evidence for a detrimental role of recurrent SDs in cortical peri-infarct zones (Ohta et al., 2001). Subsequent deterioration of the EEG in the additional course of the experiment shown in Figure 3 was linked to increases of ICP and concomitant secondary negative deflection of the DC potential.

Regional CBF in relation to striatal depolarizations

The average CBF at the two recording sites in the caudate nucleus was 66.3 ± 49.9 ml/100 g/min during control and decreased immediately after MCAO to 24.8 ± 15.6% of control. CBF measurements at the two recording sites had rather high failure rates during ongoing experiments so that we decided to average available CBF values being determined in relative temporal proximity

Table 2. Duration and amplitude of DC potential deflections in different types of depolarization

	Duration				Amplitude
	Decrease S – M (min)	Recovery M – E (min)	Recovery/decrease S – M/M – E	Total (min)	Total S – M (mV)
Early SDs ($n = 5$)	2.7 ± 1. 6	3.5 ± 1.2	2.1 ± 1.9	6.2 ± 1.6	22.6 ± 4.0
Late SDs ($n = 14$)	1.4 ± 0.8	3.5 ± 0.9	3.3 ± 3.1	4.9 ± 0.9	23.5 ± 4.4
Early LDs($n = 4$)	4.2 ± 2.3	45.2 ± 9.8	12.1 ± 4.6	49.4 ± 11.5	33.0 ± 5.1
Late LDs ($n = 5$)	33.9 ± 40.7	43.1 ± 31.4	4.6 ± 7.3	77.0 ± 63.1	18.6 ± 11.1
TD ($n = 12$)	>180				

Values are mean ± SD. The duration of the decrease of the DC potential was calculated using the time lag between the start point (S) and negative peak (M), and the duration of the recovery was calculated using the time lag between M and the end point (E) (see also Fig. 4). The amplitude of the DC potential was calculated using the voltage difference between the start point and negative peak.

Table 3. CBF in the caudate nucleus: relationship to transient depolarizations

	Control (ml/100 g/min)	After MCAO (ml/100 g/min)	Change (percentage of control)
SD ($n = 8$)	59.4 ± 19.8	26.2 ± 17.0	51.5 ± 48.0
LD ($n = 7$)	54.3 ± 14.9	18.5 ± 8.4	37.3 ± 22.8

Values are mean ± SD. Platinum electrodes measured CBF using hydrogen clearance. Values were obtained in relative temporal proximity (±1 h) to individual depolarizations. Note that CBF was not determined in proximity to all transient depolarizations.

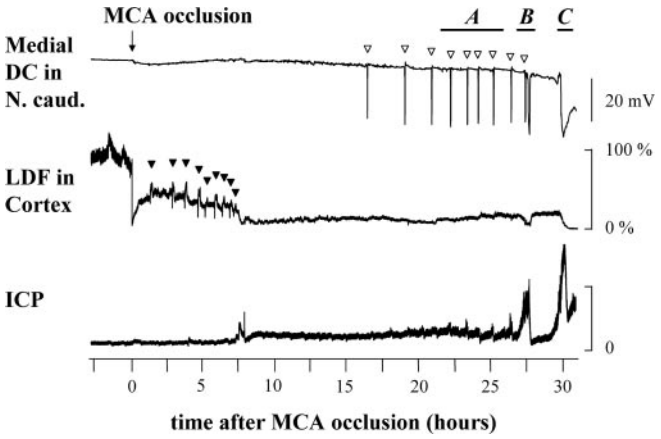

Figure 6. Simultaneous recordings of ICP, DC potential in the caudate nucleus, and LDF in the cortex before and after permanent MCAO. Views of segments A, B, and C are shown at a higher resolution in Figure 7. Note in this example repetitive depolarizations on DC recording in the caudate nucleus defined in our study as SD (open arrowheads) appearing 16–27 h after MCAO. During this phase, ICP rises slowly but continuously, interrupted by brief steeper elevations that seem temporally related to generation of individual waves of SD. Subsequent dramatic rise of ICP resulted in permanent depolarization in the caudate nucleus, presumably documenting a malignant course with herniation and brain death at this late stage. Note also repetitive transient deflections on the cortical LDF recording (closed arrowheads). Such deflections of regional CBF are typical correlates of waves of SD in not yet severely compromised tissue.

(±1 h) to transient depolarizations of the various kinds. This analysis showed that CBF decreased in proximity of TDs to ~33% of control and in proximity of LDs to ~37%, whereas decreases in proximity of SDs amounted only to ~51% (Table 3).

Malignant course: relationship to ICP and ischemic depolarizations

Our results show that SD generation is common in gray matter structures after MCAO and thus a multifocal process. This fact was visualized best in a particular experiment shown in Figure 6. In this example, repetitive transient deflections can be seen early after MCAO on the trace with cortical LDF recording. These brief deflections of regional CBF comprise a short phase of hypoperfusion followed by a longer phase of hyperperfusion. They are typical correlates of waves of SD in not yet severely compromised tissue. In the example, LDF deteriorates with repetitive deflections, and the amplitude of the CBF response is more and more reduced, documenting worsening of conditions in the cortical region studied. At a later stage, repetitive SDs can be detected on the trace with DC recording in the medial caudate nucleus. The example in Figure 6 points again to the close relationship between raised ICP in the prolonged course of MCAO and the initiation of depolarizations at later stages. Repetitive depolarizations in the medial caudate nucleus appeared 16–27 h after MCAO. During this phase, ICP increased slowly but continuously, interrupted by brief steeper elevations, and individual waves of SD were generated almost at the same time intervals as these steeper ICP rises. An unambiguous causal connection between ICP rise, LDF decline, and initiation of SDs, however, cannot be easily depicted (A in Fig. 6; enlarged image in Fig. 7*A*). In the successive episode (B in Fig. 6; enlarged image in Fig. 7*B*), the ICP rise was mirrored by a decline of cortical LDF, and two depolarizations (the first being an SD and the second an LD) were generated with some time delay in the caudate nucleus. The subsequent decrease of ICP and increase of LDF was followed by repolarization. At the final stage of this experiment (C in Fig. 6; enlarged image in Fig. 7*C*), a dramatic rise of ICP resulted in a further decline not only of cortical blood flow as documented by the decrease in LDF but also of cerebral perfusion pressure (CPP; calculated on-line as the difference between BP and ICP). At CPP values of ~50 mmHg, cerebral perfusion seemed to be not any more able to meet the energy requirements of the tissue. As a result, TD developed. The decreases of ICP and BP soon thereafter are presumably correlates of transtentorial herniation, documenting the final stage of this malignant course.

Discussion

Incidence and propagation of ischemic depolarizations in striatum

Our study characterizes for the first time in the striatum different types of ischemic depolarizations induced after MCAO in cats. The choice of the cat model allowed us to compare with former studies in which we were able to differentiate between various types of ischemic depolarizations in cortical regions (Saito et al., 1997; Ohta et al., 1997, 2001). In essence, the three types of depolarization described in our study exist also in the cortex, and the finding that ischemic SDs are generated in regions with prolonged or persistent depolarization seems to be common in this model for subcortical as well as cortical gray matter. This is presumably also true for rat models of focal ischemia, because generation of the various types of depolarization have been described in these models for cortical regions (Nedergaard and Hansen, 1993; Nallet et al., 1999). For the striatum, one report exists that has described SD generation in a rat model of focal ischemia (Wahl et al., 1994). The finding of SD generation in the striatum is not surprising, because it is well known that SD can be induced not only in cortical but also in subcortical regions such as the hippocampus or striatum (for review, see Somjen, 2001). Interestingly, waves of SD have been described to even travel between

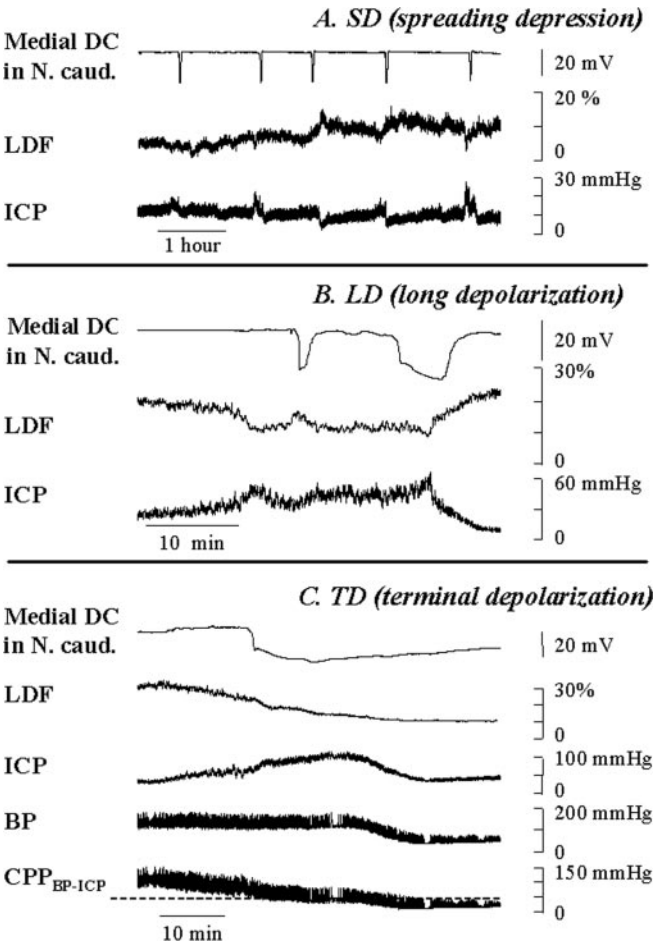

Figure 7. Magnified view of segments A, B, and C in Figure 6 of ICP, DC potential in the caudate nucleus, and LDF in the cortex. Top, Recurring SDs in the caudate nucleus and concomitant, almost simultaneous repetitive elevations of ICP. The cortical LDF recording did not show a clear correlation to ICP elevations. Middle, Transient steep rise of ICP shortly before reaching the final stage of the experiment (see bottom panel). This ICP elevation is paralleled by a transient decrease of LDF. With a delay of a few minutes, an SD followed by an LD is to be observed on the medial DC channel in the caudate nucleus. Bottom, Recordings at the final stage in relation to the decline of the CPP. For on-line recording, we calculated the CPP as the difference between BP and ICP (CPP_{BP-ICP}). TD develops in the experiment at the CPP of 50–60 mmHg, when LDF is decreased to ~20% of control. Subsequent further rise of ICP presumably leads to transtentorial herniation, resulting in a drop of ICP and BP.

the caudate nucleus and cortex (Vinogradova et al., 1991), a finding that may possess some significance in so far as some SDs seen in cortical peri-infarct zones may originate in the striatum, a region known to usually undergo severe ischemia after MCAO (Globus et al., 1988; Butcher et al., 1990). The question arises, however, whether our data support the assumption that depolarizations in the striatum, and in particular SDs, play a similar detrimental role in peri-infarct zones in the striatum as is well accepted for cortical peri-infarct SDs (Gill et al., 1992; Iijima et al., 1992; Nedergaard and Hansen, 1993; Busch et al., 1996; Hossmann, 1996; Takano et al., 1996; Saito et al., 1997; Strong et al., 2000; Ohta et al., 2001). In this context, the more general question in dispute is whether a penumbra exists at all in the striatum.

Transient ischemic depolarizations: evidence for a striatal penumbra?

The striatum has been referred to as an "ischemic core" region that exhibits very low residual CBF after MCAO (Butcher et al., 1990). This low flow has been explained by the fact that lenticulostriate arteries, which are end arteries without collateral reserve, supply the striatum (Shigeno et al., 1985). Our CBF measurements in the striatum, although heterogeneous, do not fully support this notion. The mean reduction of CBF to 24.8 ± 15.6% of control immediately after occlusion was severe; however, CBF values of 37.3 ± 22.8 and 51.5 ± 48.0 obtained in the later course of MCAO along with transient depolarizations of the LD or SD type, respectively, show that some potential for spontaneous CBF recovery exists in the striatum. This microcirculatory improvement may be linked to ischemic release of mediators of vasodilatation such as adenosine or nitric oxide that are known to increase during ischemia (Hagberg et al., 1987; Matsumoto et al., 1992; Malinski et al., 1993; Phillis et al., 1996). The opening of collateral channels seems to play a minor role, because end arteries supply this brain region (see above). Continuous CBF measurement using LDF or regional techniques such as positron emission tomography or perfusion-weighted MRI would obviously help to clarify this question, but presumably because of insufficient resolution, detailed investigations of gradual CBF changes in subcortical regions are so far missing. Nevertheless, there is evidence that residual CBF is high enough in parts of the striatum to meet the criteria for being classified "ischemic penumbra." This notion is also supported by our observation that secondary moderate elevations of ICP may drive a region into depolarization and thereby into core conditions (Fig. 3). This is most likely achieved by a secondary decrease of CBF attributable to ICP rise, and such newly generated core may give rise to the generation and propagation of SDs into surrounding regions at later time points in the course of focal ischemia.

Our electrophysiological results provide more evidence for the assumption of an ischemic penumbra in the striatum. After the original concept, penumbral zones develop failure of spontaneous electrical activity, whereas ion homeostasis and thereby structural integrity remain preserved (Astrup et al., 1981). In our experiments, the mean EEG amplitude in the caudate nucleus after MCAO was almost equally reduced at all sites to ~30% of control and tended to decrease a little more in the later course (Figs. 2, 3). Differences in EEG reduction between sites displaying TD, LD, or SD were not significant, although reduction at sites with LD and TD tended to be somewhat larger. Therefore, we argue that regions with reduction of spontaneous electrical activity and persistent reduction of the DC potential fulfill the criteria for core conditions and are to be distinguished from regions with reduction of spontaneous electrical activity alone, the latter ones being of the penumbra type with preserved ion homeostasis. Many investigators have shown peri-infarct depolarizations without identifying whether they appear in ischemic penumbra or in more peripheral zones into which they may propagate as well. Although we also consider the role of peri-infarct depolarization to be exceptionally relevant for progressive deterioration in the penumbra, such identification can be unambiguously achieved only by analysis of simultaneously obtained recordings of spontaneous electrical activity and DC potential and, if possible, by parallel recordings of CBF. Only by then can the relevance of peri-infarct depolarization for penumbral deterioration be evaluated.

Biphasic appearance of depolarizations and malignant course of focal ischemia

At subacute stages, progressive impairment in penumbral regions seems to become manifest in a secondary phase of ischemic depolarizations. Such biphasic pattern has recently been docu-

mented in an extensive study in permanent as well as in 2 h transient focal ischemia in rats (Hartings et al., 2003). In the mentioned study, the delay between the first and second phase of appearance of depolarizations was ~8 h, an observation that is comparable with our results obtained in the caudate nucleus.

We have shown in transient 3 h focal ischemia in cats that vasogenic edema formation and brain swelling play a crucial role in secondary, delayed CBF reduction and glutamate elevation after reperfusion, resulting in infarct growth and potentially in a space-occupying, malignant course with transition from focal into global ischemia (Taguchi et al., 1996; Toyota et al., 2002, 2003). Similar exacerbation has been observed after 2.5 h focal ischemia in rats and was attributed to blood–brain barrier damage and resulting edema formation (Neumann-Haefelin et al., 2000). Our present study reveals that progressive but unsteady elevation of ICP explains delayed induction of the various types of ischemic depolarizations. The mechanism by which these depolarizations are generated involves most probably a secondary reduction of regional CBF that drives some regions exhibiting penumbra conditions (spontaneous EEG reduced, DC potential preserved) into core conditions giving rise to ATP depletion, breakdown of ion homeostasis, and persistent DC potential shift of the LD or TD type. Waves of SD may be induced in such "new" ischemic cores with elevated extracellular K^+ and glutamate and will propagate into neighboring tissue (Fig. 3). Because it has been shown that peri-infarct depolarizations not only enhance energy depletion (Busch et al., 1996; Selman et al., 2004) but also impair penumbral microcirculation by reducing capillary red blood cell perfusion despite arteriolar dilatation (Pinard et al., 2002), we assume that, in a deleterious feedback cascade, cascade-like pathophysiological sequelae of electrophysiological, metabolic, and microcirculatory perturbations generate progressive infarction. The role of brain swelling and ICP rise should not be underestimated in this process. It may give rise to additional perfusional derangement resulting in the generation of new, most probably multiple cores and penumbras, and at a final stage, it may initiate transition into a global worsening being described as malignant course of infarction.

References

Astrup J, Siesjo BK, Symon L (1981) Thresholds in cerebral ischemia–the ischemic penumbra. Stroke 12:723–725.

Back T, Kohno K, Hossmann KA (1994) Cortical negative DC deflections following middle cerebral artery occlusion and KCl-induced spreading depression: effect on blood flow, tissue oxygenation, and electroencephalogram. J Cereb Blood Flow Metab 14:12–19.

Bureš J, Burešová O, Křivánek J (1974) The mechanism and applications of Leão's spreading depression of electroencephalographic acivtity. Prague: Academia.

Busch E, Gyngell ML, Eis M, Hoehn-Berlage M, Hossmann KA (1996) Potassium-induced cortical spreading depressions during focal cerebral ischemia in rats: contribution to lesion growth assessed by diffusion-weighted NMR and biochemical imaging. J Cereb Blood Flow Metab 16:1090–1099.

Butcher SP, Bullock R, Graham DI, McCulloch J (1990) Correlation between amino acid release and neuropathologic outcome in rat brain following middle cerebral artery occlusion. Stroke 21:1727–1733.

Gill R, Andine P, Hillered L, Persson L, Hagberg H (1992) The effect of MK-801 on cortical spreading depression in the penumbral zone following focal ischaemia in the rat. J Cereb Blood Flow Metab 12:371–379.

Globus MY, Busto R, Dietrich WD, Martinez E, Valdes I, Ginsberg MD (1988) Effect of ischemia on the in vivo release of striatal dopamine, glutamate, and gamma-aminobutyric acid studied by intracerebral microdialysis. J Neurochem 51:1455–1464.

Gorji A (2001) Spreading depression: a review of the clinical relevance. Brain Res Rev 38:33–60.

Graf R, Kataoka K, Rosner G, Heiss WD (1986) Cortical differentiation in cat focal ischemia: disturbance and recovery of sensory functions in corticalareas with different degrees of cerebral blood flow reduction. J Cereb Blood Flow Metab 6:566–573.

Hadjikhani N, Sanchez Del Rio M, Wu O, Schwartz D, Bakker D, Fischl B, Kwong KK, Cutrer FM, Rosen BR, Tootell RB, Sorensen AG, Moskowitz MA (2001) Mechanisms of migraine aura revealed by functional MRI in human visual cortex. Proc Natl Acad Sci USA 98:4687–4692.

Hagberg H, Andersson P, Lacarewicz J, Jacobson I, Butcher S, Sandberg M (1987) Extracellular adenosine, inosine, hypoxanthine, and xanthine in relation to tissue nucleotides and purines in rat striatum during transient ischemia. J Neurochem 49:227–231.

Hartings JA, Rolli ML, Lu XC, Tortella FC (2003) Delayed secondary phase of peri-infarct depolarizations after focal cerebral ischemia: relationship to infarct growth and neuroprotection. J Neurosci 23:11602–11610.

Higuchi T, Takeda Y, Hashimoto M, Nagano O, Hirakawa M (2002) Dynamic changes in cortical NADH fluorescence and direct current potential in rat focal ischemia: relationship between propagation of recurrent depolarization and growth of the ischemic core. J Cereb Blood Flow Metab 22:71–79.

Hossmann KA (1996) Periinfarct depolarizations. Cerebrovasc Brain Metab Rev 8:195–208.

Iijima T, Mies G, Hossmann KA (1992) Repeated negative DC deflections in rat cortex following middle cerebral artery occlusion are abolished by MK-801: effect on volume of ischemic injury. J Cereb Blood Flow Metab 12:727–733.

Leão AAP (1944) Spreading depression of activity in the cerebral cortex. J Neurophysiol 7:359–390.

Malinski T, Bailey F, Zhang ZG, Chopp M (1993) Nitric oxide measured by a porphyrinic microsensor in rat brain after transient middle cerebral artery occlusion. J Cereb Blood Flow Metab 13:355–358.

Marshall WH (1959) Spreading cortical depression of Leao. Physiol Rev 39:239–279.

Matsumoto K, Graf R, Rosner G, Shimada N, Heiss WD (1992) Flow thresholds for extracellular purine catabolite elevation in cat focal ischemia. Brain Res 579:309–314.

Mies G, Iijima T, Hossmann KA (1993) Correlation between peri-infarct DC shifts and ischaemic neuronal damage in rat. NeuroReport 4:709–711.

Nallet H, MacKenzie ET, Roussel S (1999) The nature of penumbral depolarizations following focal cerebral ischemia in the rat. Brain Res 842:148–158.

Nedergaard M, Astrup J (1986) Infarct rim: effect of hyperglycemia on direct current potential and [^{14}C]2-deoxyglucose phosphorylation. J Cereb Blood Flow Metab 6:607–615.

Nedergaard M, Hansen AJ (1993) Characterization of cortical depolarizations evoked in focal cerebral ischemia. J Cereb Blood Flow Metab 13:568–574.

Neumann-Haefelin T, Kastrup A, de Crespigny A, Yenari MA, Ringer T, Sun GH, Moseley ME (2000) Serial MRI after transient focal cerebral ischemia in rats: dynamics of tissue injury, blood-brain barrier damage, and edema formation. Stroke 31:1965–1972.

Nilsson P, Hillered L, Olsson Y, Sheardown MJ, Hansen AJ (1993) Regional changes in interstitial K^+ and Ca^{2+} levels following cortical compression contusion trauma in rats. J Cereb Blood Flow Metab 13:183–192.

Ohta K, Graf R, Rosner G, Heiss WD (1997) Profiles of cortical tissue depolarization in cat focal cerebral ischemia in relation to calcium ion homeostasis and nitric oxide production. J Cereb Blood Flow Metab 17:1170–1181.

Ohta K, Graf R, Rosner G, Heiss WD (2001) Calcium ion transients in peri-infarct depolarizations may deteriorate ion homeostasis and expand infarction in focal cerebral ischemia in cats. Stroke 32:535–543.

Phillis JW, Smith-Barbour M, O'Regan MH (1996) Changes in extracellular amino acid neurotransmitters and purines during and following ischemias of different durations in the rat cerebral cortex. Neurochem Int 29:115–120.

Pinard E, Nallet H, MacKenzie ET, Seylaz J, Roussel S (2002) Penumbral microcirculatory changes associated with peri-infarct depolarizations in the rat. Stroke 33:606–612.

Reinoso-Suárez F (1961) Topographischer Hirnatlas der Katze. Darmstadt, Germany: E. Merck AG.

Röther J, de Crespigny AJ, D'Arceuil H, Iwai K, Moseley ME (1996) Recov-

ery of apparent diffusion coefficient after ischemia-induced spreading depression relates to cerebral perfusion gradient. Stroke 27:980–986.

Saito R, Graf R, Hubel K, Fujita T, Rosner G, Heiss WD (1997) Reduction of infarct volume by halothane: effect on cerebral blood flow or perifocal spreading depression-like depolarizations. J Cereb Blood Flow Metab 17:857–864.

Selman WR, Lust WD, Pundik S, Zhou Y, Ratcheson RA (2004) Compromised metabolic recovery following spontaneous spreading depression in the penumbra. Brain Res 999:167–174.

Shibata M, Siegfried B, Huston JP (1977) Miniature calomel electrode for recording DC potential changes accompanying spreading depression in the freely moving rat. Physiol Behav 18:1171–1174.

Shigeno T, McCulloch J, Graham DI, Mendelow AD, Teasdale GM (1985) Pure cortical ischemia versus striatal ischemia. Circulatory, metabolic, and neuropathologic consequences. Surg Neurol 24:47–51.

Somjen GG (2001) Mechanisms of spreading depression and hypoxic spreading depression-like depolarization. Physiol Rev 81:1065–1096.

Strong AJ, Venables GS, Gibson G (1983) The cortical ischaemic penumbra associated with occlusion of the middle cerebral artery in the cat: 1. Topography of changes in blood flow, potassium ion activity, and EEG. J Cereb Blood Flow Metab 3:86–96.

Strong AJ, Smith SE, Whittington DJ, Meldrum BS, Parsons AA, Krupinski J, Hunter AJ, Patel S, Robertson C (2000) Factors influencing the frequency of fluorescence transients as markers of peri-infarct depolarizations in focal cerebral ischemia. Stroke 31:214–222.

Strong AJ, Fabricius M, Boutelle MG, Hibbins SJ, Hopwood SE, Jones R, Parkin MC, Lauritzen M (2002) Spreading and synchronous depressions of cortical activity in acutely injured human brain. Stroke 33:2738–2743.

Taguchi J, Graf R, Rosner G, Heiss WD (1996) Prolonged transient ischemia results in impaired CBF recovery and secondary glutamate accumulation in cats. J Cereb Blood Flow Metab 16:271–279.

Takano K, Latour LL, Formato JE, Carano RA, Helmer KG, Hasegawa Y, Sotak CH, Fisher M (1996) The role of spreading depression in focal ischemia evaluated by diffusion mapping. Ann Neurol 39:308–318.

Toyota S, Graf R, Valentino M, Yoshimine T, Heiss WD (2002) Malignant infarction in cats after prolonged middle cerebral artery occlusion: glutamate elevation related to decrease of cerebral perfusion pressure. Stroke 33:1383–1391.

Toyota S, Graf R, Valentino M, Yoshimine T, Heiss WD (2003) Prediction of malignant infarction: perifocal neurochemical monitoring following prolonged MCA occlusion in cats. Acta Neurochir Suppl 86:153–157.

Vinogradova LV, Koroleva VI, Bures J (1991) Re-entry waves of Leao's spreading depression between neocortex and caudate nucleus. Brain Res 538:161–164.

Wahl M, Schilling L, Parsons AA, Kaumann A (1994) Involvement of calcitonin gene-related peptide (CGRP) and nitric oxide (NO) in the pial artery dilatation elicited by cortical spreading depression. Brain Res 637: 204–210.